Heat Convection and Transport Barriers in Low-Magnetic-Shear Rijnhuizen Tokamak Project Plasmas

P. Mantica,[2] G. Gorini,[3,2] G. M. D. Hogeweij,[1] N. J. Lopes Cardozo,[1] and A. M. R. Schilham[1]

[1]*FOM Instituut voor Plasmafysica "Rijnhuizen," Associatie Euratom-FOM, Trilateral Euregio Cluster, P.O. Box 1207, 3430 BE Nieuwegein, The Netherlands*
[2]*Istituto di Fisica del Plasma "P. Caldirola," Associazione Euratom-ENEA-CNR, Milano, Italy*
[3]*INFM and Dipartimento di Fisica "G. Occhialini," Università degli Studi di Milano-Bicocca, Milano, Italy*
(Received 26 June 2000)

Layers of reduced electron heat transport ("transport barriers") have been observed in the Rijnhuizen Tokamak Project when the plasma is dominantly heated by electron cyclotron heating (ECH). Experiments into the properties of the transport barriers are reported. Modulation of the ECH power was used to probe electron heat transport in the barriers by means of propagating electron temperature perturbations. The observed propagation shows that transport inside the barriers is dominated by heat convection. This convection is inward, i.e., up the temperature gradient.

PACS numbers: 52.55.Fa, 52.25.Fi, 52.50.Gj

Transport barriers are an area of active research in magnetically confined plasmas because of their beneficial effect on energy confinement. Internal transport barriers (ITB) are by now commonly observed in tokamaks in the electron and/or ion channel under a variety of experimental conditions [1–6]. Small tokamaks are no exception: the Rijnhuizen Tokamak Project (RTP) has demonstrated an electron transport dominated plasma regime where electron thermal transport barriers were observed in plasmas dominantly heated by electron cyclotron heating (ECH) [7]. A "shell model" has been developed for these plasmas, where such electron ITBs are assumed to be layers of reduced electron thermal diffusivity (χ_e) located near low order rational magnetic surfaces and whose width in space is determined by the local magnetic shear [8]. This model shares some of the features of electron ITBs observed in larger tokamaks and is currently being tested on JET electron ITBs [9]. While ITBs are typically a transient event in large tokamaks, the ITBs in RTP are stationary for tens of energy confinement times and several current diffusion times, which makes them suitable for detailed investigation.

In this Letter, we report the results of experiments performed in order to probe the transport properties of RTP transport barriers [10]. Modulated ECH (MECH) was used to provide a localized source of electron temperature (T_e) perturbations that propagate across the barriers. Standard Fourier analysis of the T_e time traces provides information on the amplitude (A) and phase lag (φ) of the heat wave at several harmonics of the modulation frequency. This multifrequency information can in turn be used to investigate the χ_e profile as well as deviations from a simple diffusive behavior [11]. Moreover, MECH provides a way to determine the power deposition radius (ρ_{dep}) from the location of the minimum φ. The combined steady-state and MECH evidence provides a much more stringent test of the barrier transport properties than either evidence alone.

The RTP tokamak ($R = 0.72$ m, $a = 0.16$ m) was operated for transport studies and equipped with advanced diagnostics. Time resolved measurements of T_e and electron density (n_e) were taken with a 15-channel electron cyclotron emission (ECE) radiometer and a 16-chord microwave interferometer. High spatial resolution was obtained with a Thomson scattering system measuring T_e and n_e on a vertical chord with a spatial resolution $\Delta z = 2.6$ mm. MECH from a 110 GHz, 350 kW gyrotron (second harmonic X-mode) is used to induce T_e perturbations. The same gyrotron provides the heating required for these experiments.

Figure 1 illustrates the central T_e response to shot-to-shot variations of ρ_{dep} in conditions of dominant ECH power ($P_{ECH}/P_{OH} > 3$) [7]. The deposition was located at the low field side and varied by varying the toroidal magnetic field. The salient feature of these measurements, as reported in [7,8], is the discontinuous response of the T_e profile to a continuous variation of ρ_{dep}. Five plateaus
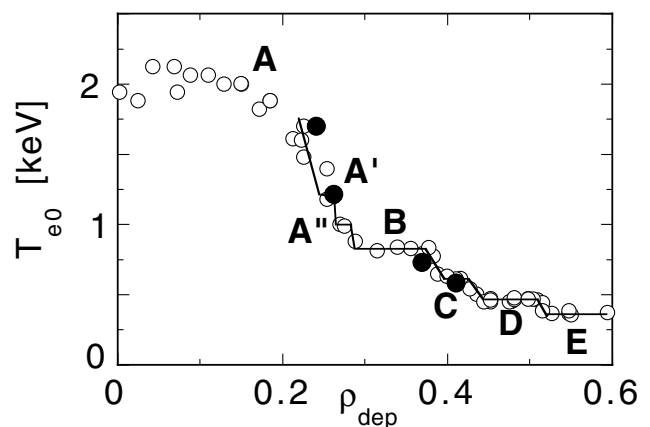
FIG. 1. Central T_e vs ρ_{dep} for a set of similar discharges [$I_p = 80$ kA, $q_a \sim 5$, $n_e(0) = 4 \times 10^{19}$ m^{-3}] in which ρ_{dep} was increased in small steps from shot to shot. The solid dots mark the discharges where the ECH power was modulated. The line is a guide to the eye. The data have been slightly revised with respect to those reported in Refs. [7,8] by using improved diagnostic information.

(labeled with letters from *A* to *E*), in which T_e is rather insensitive to changes in ρ_{dep}, are separated by sudden transitions occurring for small changes of ρ_{dep}. These transitions have been correlated with the loss of low order rational magnetic surfaces (i.e., 1, 2, 2.5, 3) from the plasma [8]. Two intermediate plateaus, labeled A' and A'' have been identified, in which q_{min} is between 1 and 4/3, and between 4/3 and 3/2, respectively [12]. Figure 2 illustrates the T_e profile shapes observed in the different plateaus. Both the behavior of Fig. 1 and the T_e profiles of Fig. 2 have been successfully reproduced using the shell model [8].

Although only one ECH power source was available for these experiments, it was possible to propagate heat waves in some ECH dominated plasmas by modulating the ECH power in time with a high duty cycle ($d_c \approx 85\%$). About 50 modulation cycles were used in order to produce *A* and φ profiles at three harmonics of the MECH frequency ($\omega/2\pi = 310$ Hz). Figure 3 shows a comparison between two discharges with $d_c = 0.15$ (left) and 0.85 (right). The first one is a quasi-Ohmic discharge; the second one is ECH dominated and belongs to the A' plateau. As expected, there is a clear difference in the T_e and *q* profiles. The latter were calculated from the measured T_e and n_e profiles, assuming neoclassical resistivity and correcting for the bootstrap current. More striking is the difference in the MECH data. In the low d_c case, the behavior of the *A* and φ profiles has the usual "diffusive" features: the amplitude decays and the modulation phase lag increases, moving away from the heat source (ρ_{dep}) so that the locations of the peak amplitudes and minimum phases coincide. In the high d_c case, in contrast, the data show an inward shift of the amplitude peak at first harmonic. This feature gradually disappears at higher harmonics, the third one presenting a standard diffusive pattern. Even the first harmonic phase profile is not immune from nondiffusive features: diffusive transport requires φ to increase with

frequency at ρ_{dep} and elsewhere; instead, a larger first harmonic φ value relative to the other harmonics is found in the region just outside ρ_{dep}.

A similar behavior is found as the ρ_{dep} location is moved outward. This was investigated by modulating the ECH power in four of the discharges belonging to the ρ_{dep} scan of Fig. 1. An inward shift of the first harmonic *A* peak relative to ρ_{dep} is clearly observed in all four cases (see Fig. 4). Again, the shift disappears at higher harmonics.

The above observations are typical of the presence of a "heat pinch," i.e., an inward convective component in the modulated heat flux [11]. We have investigated two alternative possibilities. First, spurious ECH power deposition cannot explain the observations since its effect would persist at higher harmonics. Second, a strong χ_e gradient can, in principle, mimic "convective" propagation of T_e perturbations [11]. However, quantitative simulations have shown that a χ_e gradient still compatible with the high harmonic data would yield a much lower convective-like effect at low harmonics than measured.

Having demonstrated the presence of the heat pinch, we now consider its cause. Since the convective propagation is not seen with low d_c ECH, the ECH power cannot be the direct cause of the heat pinch. We therefore conclude that

FIG. 2. T_e profiles measured with ECE (large symbols) and Thomson scattering (small symbols, not available for *B*) for the four MECH discharges marked in Fig. 1. Negative ρ values refer to the inboard (ECE) and downward (TS) halves of the plasma. The ECH resonant surfaces are marked by vertical lines.
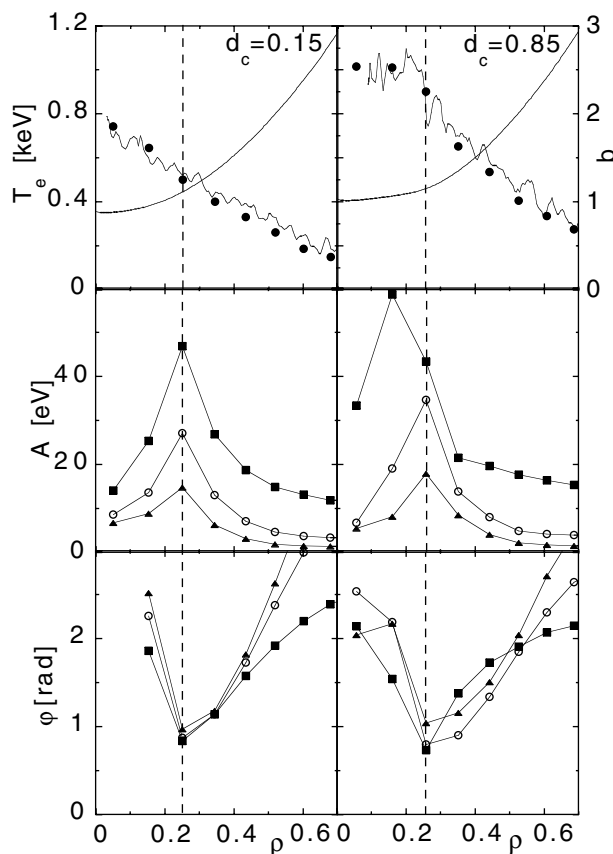
FIG. 3. T_e and *q* profiles and MECH amplitude and phase profiles at three harmonics for two similar discharges with different MECH d_c: $d_c = 0.85$ (r19980616.024, right column) and $d_c = 0.15$ (r19980616.025, left column). Plasma parameters: $I_p = 80$ kA, $q_a \sim 5$, $n_e(0) = 5 \times 10^{19}$ m^{-3}, $\rho_{dep} = 0.25$.
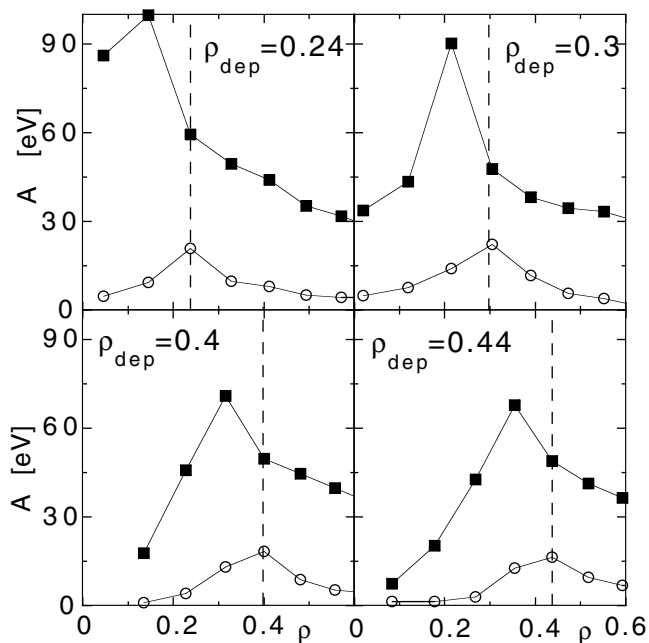
FIG. 4.   MECH amplitude profiles at first (■) and third (○) harmonics for the four MECH discharges marked in Fig. 1. The ρ_{dep} locations are marked with vertical lines.

the heat pinch is caused by changes in plasma parameters or profiles, induced by the ECH. There is interesting information in the time evolution of the T_e oscillations after switch-on of the MECH. This shows that the time scale for the onset of the heat pinch is longer than the energy confinement time (3 ms) and comparable to the current diffusion time (10 ms). This suggests that the magnetic shear may be a key factor for the onset of the heat pinch.

A closer inspection of the steady-state T_e profiles of Fig. 2 reveals that a heat pinch component must also be present in the time averaged heat flux. One can note that the maximum T_e value is always located inside ρ_{dep} (note that ρ_{dep} is determined consistently from modulated ECE data, thus ruling out systematic errors in ρ_{dep} relative to the ECE profile). This feature is particularly evident in the plateau A case, where T_e is significantly peaked on axis (this feature is not clearly seen in the Thomson scattering data because the diagnostic laser beam misses the plasma axis by up to 2 cm, depending on the Shafranov shift). Detailed power balance analysis of these discharges shows that the Ohmic power cannot account for this feature. Thus, the steady-state T_e profiles are also in qualitative agreement with a heat pinch component in the heat flux.

To model the heat pinch, we assume that the electron heat flux consists of two components, $-q_e = n_e \chi \nabla T_e + n_e U T_e$ [11]. The first component is diffusive and is assumed to dominate over the pinch term, except in a plasma layer located near ρ_{dep}, where the heat pinch component is dominant and pumps heat uphill against the T_e gradient. The heat pinch velocity (U) and heat diffusivity (χ_e) profiles required to reproduce both steady-state and MECH data are investigated with the help of 1D full transport

simulations using the ASTRA code [13]. The code solves the coupled force balance and transport equations of tokamak plasmas. Of relevance for these experiments are the electron heat transport and the current diffusion equations. Since ECH only heats the electrons directly, and the coupling between the electron and ion fluids is very weak in RTP ($\tau_{ei} \gg \tau_E$), the ion energy balance does not play a significant role in this experiment. The n_e profile and the main plasma parameters are taken from the experiment, together with the ECH power deposition profile.

For the simulations the following strategy was followed. We recall that the shell model described in [8,12] gives a good match to the steady-state data presented in Figs. 1 and 2. In this model, χ_e is a function of q only, with regions of low χ_e (barriers) situated near $q = 1, 4/3, 3/2, 2, \ldots$, separated by regions with uniform high χ_e (typically 10 m²/s). A single function $\chi_e(q)$ is capable of describing the wide range of T_e profiles in Fig. 2.

However, it is clear that this model cannot reproduce the MECH data, as it does not feature heat pinch type barriers. Also, the slopes of the A and φ profiles at high harmonics show that χ_e is low in the plasma center and increases with radius. It is also clear that, as far as the steady-state data is concerned, the diffusive barriers in the model could be replaced by layers of inward heat convection; in general, in steady state the two transport mechanisms cannot be distinguished. Only where a power balance, assuming pure diffusive transport, leads to negative χ_e does the necessity for a convective component arise. In fact, as noted previously, the new, more accurate determination of ρ_{dep} does place the steep T_e gradient inside ρ_{dep}, calling for convective type barriers also on the basis of steady-state data.

An obvious step was therefore to replace the diffusive barriers in the shell model by layers of inward convection. As in the original shell model, these layers are coupled to intervals of q, rather than being defined in terms of ρ. Indeed, it was possible to recover the T_e profile shapes and the stair-step behavior of $T_e(0)$ as a function of ρ_{dep}. However, since there still needs to be a background diffusive transport (of which a profile must be provided), with both conduction and convection (the barriers) as variables in the simulation, the sparse MECH data was insufficient to uniquely determine all of the free parameters. Moreover, one cannot exclude the possibility that both the heat pinch layers and the conductive barriers play a role, in which case the number of free parameters is even larger.

We therefore chose to model single discharges for which MECH data were available. Only one barrier, i.e., the most prominent one, was modeled in these simulations, of which the aim is to match the T_e profile as well as the phase and amplitude data of the MECH experiment. In Fig. 5 the results of such simulation for the MECH discharge belonging to plateau A ($\rho_{\text{dep}} = 0.24$) are compared to the experimental data. The transport coefficients and ECH profile assumed are also shown. As a boundary condition the outermost T_e measurement ($\rho = 0.72$) was used. It was found that a heat pinch velocity with peak value
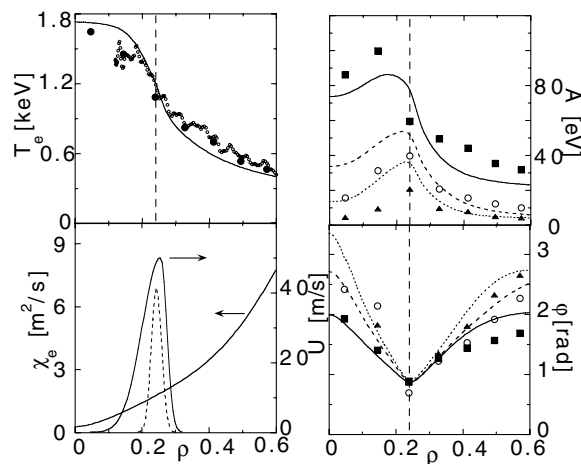
FIG. 5.   Simulated (lines) and experimental (symbols) profiles of T_e, MECH amplitudes, and phases at three harmonics for $\rho_{dep} = 0.24$ (plateau A). The χ_e, U, and P_{ECH} profiles (dashed line, in a.u.) used in the simulation are also shown.

$U = 50$ m/s, localized in a narrow region of the plasma, can match the main features of the data. Simulations were done also for the other three MECH discharges in Fig. 4, using U peak values in the range $60-80$ m/s and resulting in similar agreement between simulation and data.

We note first that a layer of rather strong heat convection is indeed capable of reproducing the inward shift of the amplitude maximum at the first harmonic of the modulation frequency and the disappearance of this shift with increasing frequency. Also the position of the steep T_e gradient is well reproduced. However, the details of the T_e profile shape are not well reproduced, and also the high slopes of the second and third harmonic amplitude inside ρ_{dep}. The latter feature, on the other hand, is independent of the existence of a heat pinch (compare the high and low d_c cases in Fig. 3). These mismatches between data and simulation can be recovered by turning to more elaborate transport models, where the χ_e value seen by the perturbation (χ_e^{pert}) is allowed to deviate from the power balance χ_e (χ_e^{PB}) [14]. We did test explicit dependencies, e.g., χ_e as a function of ∇T_e, and we have verified that the main features of the heat pinch velocity profile are not sensitive to the use of more elaborate models. On this basis we decided to focus on the heat pinch issue and present results based on the simplest model yielding the U profile.

In summary, the simulations showed that the position of the steep ∇T_e barrier relative to the radius of power deposition, as well as the inward shift of the amplitude maximum with respect to the phase minimum of MECH data, calls for a layer of inward heat convection with a width of 10% of the minor radius, centered on the ECH deposition radius, and with a maximum pinch velocity of (about) 50 m/s. A model featuring such convective barriers at simple rational q-values does reproduce the stair-step behavior of $T_e(0)$ vs ρ_{dep}, but such a model has too many free parameters for the present data set to uniquely determine those barriers.

Early results from DIII-D [15] suggested the presence of a heat pinch effect in off-axis ECH plasmas. The present results from RTP confirm the DIII-D results, and place the heat pinch issue in the more general context of the existence of transport barriers in tokamak plasmas.

In general, all results concerning the existence of internal transport barriers in tokamaks in the presence of low or negative shear are based on steady-state analysis, so the idea that such barriers are regions of low thermal diffusivity is in fact an assumption *a priori*. The RTP results suggest that convection may play an important role in electron ITBs and set an experimental paradigm for its investigation.

Concerning the question of what could be the microscopic mechanism giving rise to the heat pinch, this is still completely open. A few theoretical models address the issue of heat convection [16–18], and a test of some of them against the present data is in progress.

In conclusion, electron heat transport barriers in RTP plasmas with dominant ECH behave nondiffusively when probed by heat waves from modulated ECH. The experimental evidence suggests the existence of heat pinch layers pumping heat inward against the T_e gradient.

[1] F. M. Levinton *et al.,* Phys. Rev. Lett. **75**, 4417 (1995).
[2] E. J. Strait *et al.,* Phys. Rev. Lett. **75**, 4421 (1995).
[3] S. Ishida *et al.,* Phys. Rev. Lett. **79**, 3917 (1997).
[4] C. Gormezano *et al.,* Phys. Rev. Lett. **80**, 5544 (1998).
[5] S. Gunter *et al.,* Phys. Rev. Lett. **84**, 3097 (2000).
[6] G. T. Hoang *et al.,* Phys. Rev. Lett. **84**, 4593 (2000).
[7] N. J. Lopes Cardozo *et al.,* Plasma Phys. Controlled Fusion **39**, 303 (1997).
[8] G. M. D. Hogeweij *et al.,* Nucl. Fusion **38**, 1881 (1998).
[9] A. M. R. Schilham *et al.,* in Proceedings of the 27th Conference on Controlled Fusion and Plasma Physics, Budapest, 2000 [European Physical Society, Innsbruck (to be published)].
[10] P. Mantica *et al.,* in Proceedings of the 27th Conference on Controlled Fusion and Plasma Physics, Budapest, 2000 (Ref. [9]).
[11] A. Jacchia *et al.,* Phys. Fluids B **3**, 3033 (1991).
[12] M. R. de Baar *et al.,* Phys. Plasmas **6**, 4645 (1999).
[13] G. V. Pereverzev *et al.,* Max-Planck-IPP Report IPP 5/42, 1991.
[14] N. J. Lopes Cardozo, Plasma Phys. Controlled Fusion **37**, 799 (1995).
[15] T. C. Luce *et al.,* Phys. Rev. Lett. **68**, 52 (1992).
[16] F. Porcelli *et al.,* Phys. Rev. Lett. **82**, 1458 (1999).
[17] J. Weiland and H. Nordman, Phys. Fluids B **5**, 1669 (1993).
[18] A. Thyagaraia, in *Proceedings of the 26th EPS Conference on Controlled Fusion and Plasma Physics, Maastricht, 1999* (European Physical Society, Innsbruck, 1999), Vol. 23J, p. 145.